Journal of Chemical Health Risks

www.jchr.org

JCHR (2023) 13(4), 940-949 | ISSN:2251-6727

Preparation, Characterization and Cytotoxicity Evaluation of Starch-Based on Electrospun Nanofibrous Scaffold Incorporated with Bioactive Compound from *Mollugo Nudicaulis*

Siva Shankar Raj[1], Mani Panagal[2*]

[1,2*]Department of Biotechnology, Annai College of Arts and Science (Affiliated by Bharathidasan University), Kovilacheri, Tamil Nadu 612503, India.

***Corresponding Author:** Mani Panagal

(Received: 02 September 2023 Revised: 14 October Accepted: 07 November)

KEYWORDS

Mollugo nudicaulis; 12-(10-carboxydecanoyloxy)-12-oxododecanoic acid; Starch nanofibers; Electrospinning; Cytotoxicity analysis.

ABSTRACT:

This research manuscript details the fabrication and characterization of starch-based electrospun nanofibrous scaffolds enriched with 12-(10-carboxydecanoyloxy)-12-oxododecanoic acid (Compound-1), sourced from the ethanolic extract of *Mollugo nudicaulis*. Varying concentrations of Compound-1 (0%, 20%, 30%, and 40% v/v) were incorporated into starch solutions, which were subsequently transformed into nanofibers using electrospinning. The resulting nanofibers were comprehensively analyzed for morphology, size distribution, thermal stability, FT-IR spectra, and cytotoxicity potential. The nanofibers loaded with Compound-1 exhibited consistent and uniform morphology, with average diameters falling within the range of 76 to 98 nm. Remarkably, the incorporation of Compound-1 led to an improvement in the thermal stability of the nanofibers when compared to the unencapsulated Compound-1. FT-IR analysis further confirmed interactions between the starch matrix and Compound-1. Most notably, nanofibers loaded with 40% Compound-1 demonstrated significantly enhanced viability in HaCat cells. These findings suggest that the developed starch-based electrospun nanofibrous scaffolds, enriched with Compound-1 from Mollugo nudicaulis, possess promising potential as bioactive nanomaterials for various biomedical applications. However, it is essential to conduct further in vitro and in vivo studies to validate these initial observations.

1. INTRODUCTION

Nanofibrous scaffolds have undoubtedly revolutionized the landscape of biomaterials, standing out as exceptional materials that have piqued the curiosity and enthusiasm of both scientists and healthcare practitioners. These structures possess a remarkable set of attributes that set them apart in the realm of biomedical materials. Their most notable features include a high surface area-to-volume ratio, tunable porosity, and the capacity to closely mimic the natural extracellular matrix (ECM) of living tissues. These characteristics, in particular, make nanofibrous scaffolds highly versatile and tailor-made for a wide range of biomedical applications [1]. Tissue engineering and regenerative medicine are fields that have greatly benefited from the unique properties of nanofibrous scaffolds. By offering a three-dimensional microenvironment that closely resembles the ECM, these scaffolds promote cell adhesion, proliferation, and differentiation. The porous structure encourages the exchange of nutrients and waste products, crucial for the survival and growth of new tissue. Researchers and medical professionals alike have utilized these scaffolds to repair damaged or degenerated tissues, aiding the body's natural regenerative processes [2]. Moreover, nanofibrous scaffolds have proven to be exceptional candidates for drug delivery systems. The high surface area of the nanofibers allows for the controlled release of therapeutic compounds, enabling precise dosing and timing of medication. This is particularly valuable in the treatment of chronic diseases and conditions that require sustained drug delivery over an extended period. These scaffolds not only enhance the bioavailability of the drug but also minimize potential side effects [3].

Electrospinning, in particular, has established itself as a versatile and widely adopted technique for the fabrication of nanofibrous scaffolds. This method harnesses the power of electric fields to transform polymer solutions or melts into ultrafine fibers, offering precise control over their morphology, diameter,

Journal of Chemical Health Risks

www.jchr.org

JCHR (2023) 13(4), 940-949 | ISSN:2251-6727

alignment, and other critical properties. The result is a scaffold that closely resembles the intricate and organized microstructure of native tissues [4]. One of the most exciting aspects of nanofibrous scaffolds is their ability to serve as a delivery platform for bioactive compounds. By incorporating therapeutic agents, growth factors, antimicrobial substances, or even natural extracts into these scaffolds, researchers can create innovative biomaterials that not only provide structural support but also possess specific therapeutic functions. This controlled release of bioactive compounds is a promising avenue for enhancing the bioactivity of nanofibrous scaffolds, making them even more effective in promoting tissue regeneration and delivering therapeutic agents to targeted sites within the body [5].

Enhancing the bioactivity of nanofibrous scaffolds is of paramount importance for their efficacy in biomedical applications. The incorporation of bioactive compounds, such as growth factors, antimicrobial agents, or natural extracts, can imbue these scaffolds with specific therapeutic properties. By encapsulating these compounds within the nanofibers, their controlled release can be achieved, improving the scaffolds' ability to promote tissue regeneration or deliver therapeutic agents to target sites [6].

Mollugo nudicaulis (*M. nudicaulis*), a medicinal plant, has been identified as a potential source of bioactive compounds with various pharmacological properties. In this study, particular attention is given to Compound-1, a bioactive component extracted from *M. nudicaulis*. The compound has shown promise in previous research, with potential cytotoxic and wound healing properties. Incorporating such compounds into nanofibrous scaffolds could lead to innovative biomedical materials with a wide range of applications [7].

In this context, the present research manuscript focuses on the preparation, characterization, and cytotoxicity evaluation of starch-based electrospun nanofibrous scaffolds that are enriched with 12-(10-carboxydecanoyloxy)-12-oxododecanoic acid, referred to as Compound-1, sourced from the ethanolic extract of *Mollugo nudicaulis*. This study explores the potential of these nanofibrous scaffolds as a promising platform for delivering bioactive compounds with potential biomedical applications.

2. MATERIALS AND METHODS

2.1. Preparation of Polymeric Solutions for Electrospinning

The polymeric solutions required for electrospinning were meticulously prepared using soluble potato starch, which was dissolved in a mixture of formic acid and deionized water. To create the starch solution, 5 grams of starch were carefully dissolved in a solution comprising 10 mL of formic acid and deionized water. The goal was to induce starch gelatinization, and to achieve this, the solutions were stirred for 24 hours and subsequently left to age for an additional 24 hours. Various concentrations of Compound-1, a bioactive component previously isolated from an ethanolic extract of *M. nudicaulis* by our research team, were added to the starch solution in dry form. These concentrations included 0%, 10%, 20%, and 40% v/v. Before the electrospinning process, the solutions were stirred for 15 minutes to ensure a homogenous mixture. As a control, a starch solution was also prepared without the addition of Compound-1. To ensure complete polymer dissolution, all polymeric solutions were sealed and allowed to age for 24 hours at room temperature prior to the electrospinning process.

2.2. Solution Characterization

Before commencing the electrospinning process, it was essential to measure the viscosity and conductivity of the four prepared solutions. A Brookfield Model DV-II + Pro Viscometer was employed to assess viscosity, while a Metrohm-914 Conductometer was used to determine conductivity.

2.3. Electrospinning Process

The actual production of starch nanofibers, which were intended to encapsulate Compound-1, was executed using an electrospinning setup coupled with a syringe infusion pump (KD Scientific, Model 100, Holliston, England). A 3 mL plastic syringe, fitted with a stainless-steel spinneret needle with a diameter of 0.7 mm, was employed to load the fiber-forming solution. The loading took place at a distance of 20 cm from a grounded stainless-steel collector plate. The electrospinning process occurred at room temperature (25 °C ± 2 °C), with a controlled relative humidity of 45 °C ± 2 °C achieved using a dehumidifier. The solution was pumped at a constant flow rate of 0.60 mL/h, with an applied voltage of +25.0 kV and -3.0 kV. To ensure the purity of the resulting nanofibrous sheets and facilitate drying, they were rinsed three times with water and phosphate buffer solution (PBS) before being placed at 25 °C for drying.

2.4. Physicochemical characterization of fabricated nanofibers

2.4.1. Morphology and size distribution of the nanofibers

For the evaluation of nanofiber morphology, a scanning electron microscope (SEM) was utilized (Jeol, JSM-6610LV, USA). Prior to examination, the samples were meticulously sputter-coated with a thin layer of gold to enhance imaging quality. SEM analysis was conducted

Journal of Chemical Health Risks

www.jchr.org

JCHR (2023) 13(4), 940-949 | ISSN:2251-6727

at an acceleration voltage of 10 kV, allowing for a detailed examination of the nanofiber structure. To determine the size distribution and calculate the average diameter of the nanofibers, fifty nanofibers were randomly selected from the SEM micrographs. Image analysis was facilitated using ImageJ software (version 2015), enabling precise measurements and data collection for subsequent characterization and assessment.

2.4.2. Thermal stability analysis of nanofibers

To evaluate the thermal stability of the nanofibers, a thermogravimetric analyzer (TGA) was employed, specifically the TA-60WS by Shimadzu, Kyoto, Japan. Samples, each weighing approximately 5 mg, were carefully loaded into platinum capsules. The TGA analysis involved subjecting the samples to a controlled heating rate of 10°C per minute, spanning the temperature range from 30 to 600°C, all while maintaining a consistent nitrogen flow of 50 mL/min. As a reference, an empty platinum capsule was employed. This TGA analysis enabled a thorough examination of the nanofibers' thermal behavior, providing essential insights into their stability and potential applications in varying temperature environments.

2.4.3. Fourier-transform infrared (FT-IR) analysis of nanofibers

In order to gain insights into the chemical composition of the nanofibers, as well as their individual constituents, namely soluble potato starch and compound-1, an attenuated total reflection (ATR) accessory in the form of IR-affinity equipment from Shimadzu, Japan, was employed. The analysis comprised 120 scans conducted at a spectral resolution of 4 cm−1. The scanning spanned a wide wavenumber range, extending from 4000 to 500 cm−1, all while maintaining a consistent room temperature environment (25°C ± 2°C) as recommended by previous research. This infrared spectral analysis offered valuable data on the chemical bonds and interactions present in the nanofibers and their constituents.

2.5. Analysis of Cell Viability

Cell Culture: HaCat cells were meticulously cultivated in a controlled environment with a humidified atmosphere, maintaining 5% CO2 at a stable temperature of 37°C. The cells were nurtured and expanded in T-25 flasks, employing a culture medium consisting of DMEM (Dulbecco's Modified Eagle Medium) enriched with 10% fetal bovine serum (FBS) and 1% antibiotics, specifically 100 U/mL of penicillin and 100 g/mL of streptomycin. The passage of cells was executed when they attained approximately 70% confluence, using trypsinization techniques as described by Meganathan et al. in 2021 [8]. This standard cell culture procedure ensured the optimal growth and maintenance of the HaCat cell line for subsequent experimental evaluations.

2.5.2. MTT assay

Adhering to the ISO 10993-5 standard test protocol, the electrospun nanofibrous mats underwent a comprehensive evaluation for in vitro cytotoxicity. To ensure their sterility, the specimens were subjected to a sterilization process involving immersion in 70% ethanol for a duration of 30 minutes, followed by thorough washing with sterile phosphate-buffered saline (PBS). Subsequently, HaCat cells were carefully seeded in 96-well plates, with each well containing 5× 103 cells. The growth medium employed was DMEM, which was supplemented with 10% fetal bovine serum (FBS) and 1% antibiotics, thus establishing optimal conditions for cell growth and maintenance. The culture plates were then securely housed in an incubator, maintaining a constant temperature of 37°C and 5% CO2 for a 24-hour incubation period. To assess cell viability, the colorimetric MTT (3-(4,5-dimethylthiazol-2-yl)-2,5-diphenyltetrazolium bromide) assay was performed, and the optical density (OD) was quantified at 540 nm using an ELISA reader (ELX 808), following the procedure as detailed by Palanisamy et al. in 2021 [9]. This rigorous assessment provided valuable insights into the nanofibrous mats' impact on cell viability and potential biomedical applications.

2.6. Statistical Analysis

The data derived from the experiments are systematically presented as the mean values along with their corresponding standard deviations (mean ± standard deviation, SD). To assess the significance of observed differences between two distinct groups, a rigorous statistical analysis was carried out. The analytical approach employed was a t-test, a well-established method for comparing means. The level of significance for detecting differences was established at a p-value of less than 0.05. This stringent threshold ensures that any disparities observed are statistically meaningful and not due to random variation. The application of robust statistical analysis enhances the reliability of the findings and underscores the credibility of the experimental outcomes [10].

3. RESULTS AND DISCUSSION

3.1. Solution characterization

In order to draw meaningful correlations with the outcomes of the electrospinning process, an essential step was the evaluation of the properties of the polymeric

Journal of Chemical Health Risks

www.jchr.org

JCHR (2023) 13(4), 940-949 | ISSN:2251-6727

solutions that were employed prior to the electrospinning procedure. This assessment involved the precise measurement of two crucial properties: viscosity and conductivity. The collected data and their subsequent analysis are presented in Table 1. Remarkably, the results revealed distinctive trends among the prepared solutions. Specifically, as illustrated in Figure 1 and Figure 2, the solutions containing higher concentrations of compound-1 (20% and 40%) displayed markedly elevated levels of both viscosity and conductivity. This finding underscores the influence of compound-1 on the physical properties of the polymeric solutions. The increased viscosity indicates a thicker, more viscous solution, while the heightened conductivity suggests a greater ability to conduct electrical current. These observations lay the foundation for understanding how variations in compound-1 concentration can impact the behavior and characteristics of the polymeric solutions used in the electrospinning process. Such insights are invaluable in optimizing and tailoring the electrospinning parameters for specific applications and desired nanofiber properties.

Table 1: . Prepared polymeric solution composition and weight ratio

S. No.	Samples	Weight ratio (%)	
		Starch	Compound-1
1.	0% compound-1	100	0
2.	10% compound-1	90	10
3.	20% compound-1	80	20
4.	40% compound-1	60	40

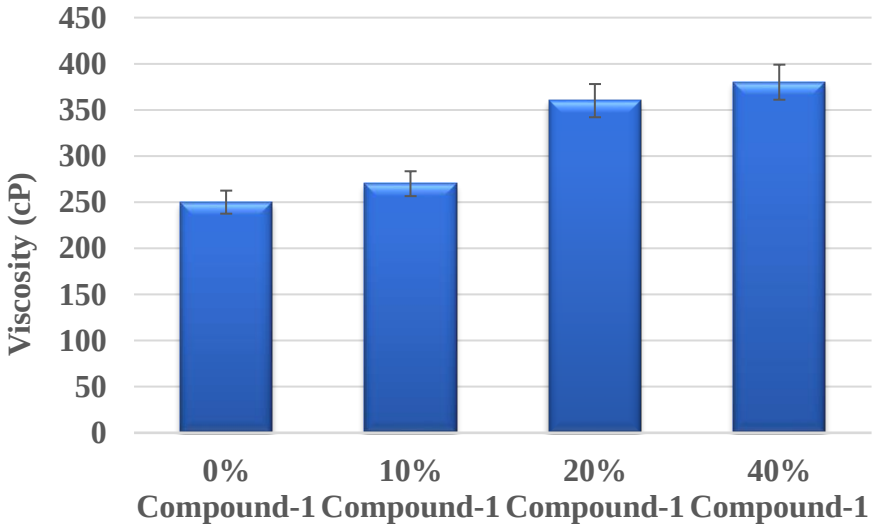

Figure 1: Viscosity of fabricated nanofibers

Journal of Chemical Health Risks
www.jchr.org
JCHR (2023) 13(4), 940-949 | ISSN:2251-6727

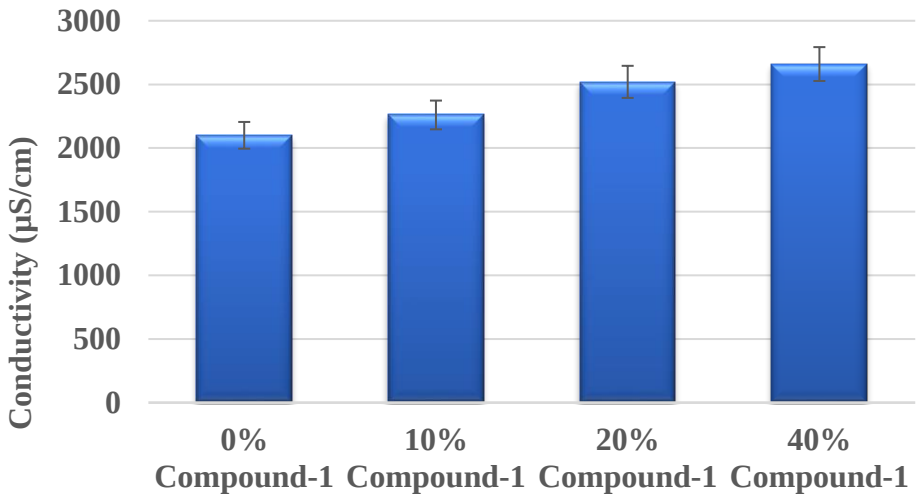

Figure 2: Conductivity of fabricated nanofibers

3.2. Physicochemical characterization of fabricated nanofibers

3.2.1. Morphology and size distribution

Figure 3 provides a vivid illustration of the intriguing diversity in the morphologies and dimensions of the nanofibers generated through the electrospinning process. Notably, nanofibers devoid of compound-1 exhibited a distinctive ribbon-like and fused structure, a feature predominantly attributed to the absence of adequate stretching during the electrospinning process. In contrast, nanofibers incorporated with varying concentrations of compound-1 (with average diameters measuring 93 nm, 76 nm, 81 nm, and 98 nm for 0%, 10%, 20%, and 40% compound-1, respectively) exhibited a remarkably distinct profile. They showcased a uniform, cylindrical, and randomly oriented structure, indicative of more rapid solvent volatilization. To align the starch molecules within the electrospinning jet, high-concentration fiber-forming solutions often require a longer tip-to-collector distance and a higher applied voltage. Despite using a relatively high starch concentration (50% w/v) in our study, it is worth noting that the solution did not exhibit a high viscosity in formic acid solvent [11]. However, the inclusion of compound-1 proved to be instrumental in enhancing the electrospinnability of the starch solution, leading to the remarkable transformation observed in the nanofiber structures.

Prior research has reported the production of ultrafine fibers characterized by beaded-fiber morphologies, often exhibiting average diameters ranging from 128 to 143 nanometers, using soluble potato starch. However, in the current study, adjustments and refinements were made to the solution parameters and electrospinning conditions. These adaptations culminated in the production of bead-less nanofibers with diameters ranging from 76 to 98 nanometers [12]. This achievement holds significant promise, particularly in the realm of wound healing applications, as it enables the controlled release of compound-1 and provides an innovative avenue for addressing critical aspects of regenerative medicine.

Journal of Chemical Health Risks

www.jchr.org

JCHR (2023) 13(4), 940-949 | ISSN:2251-6727

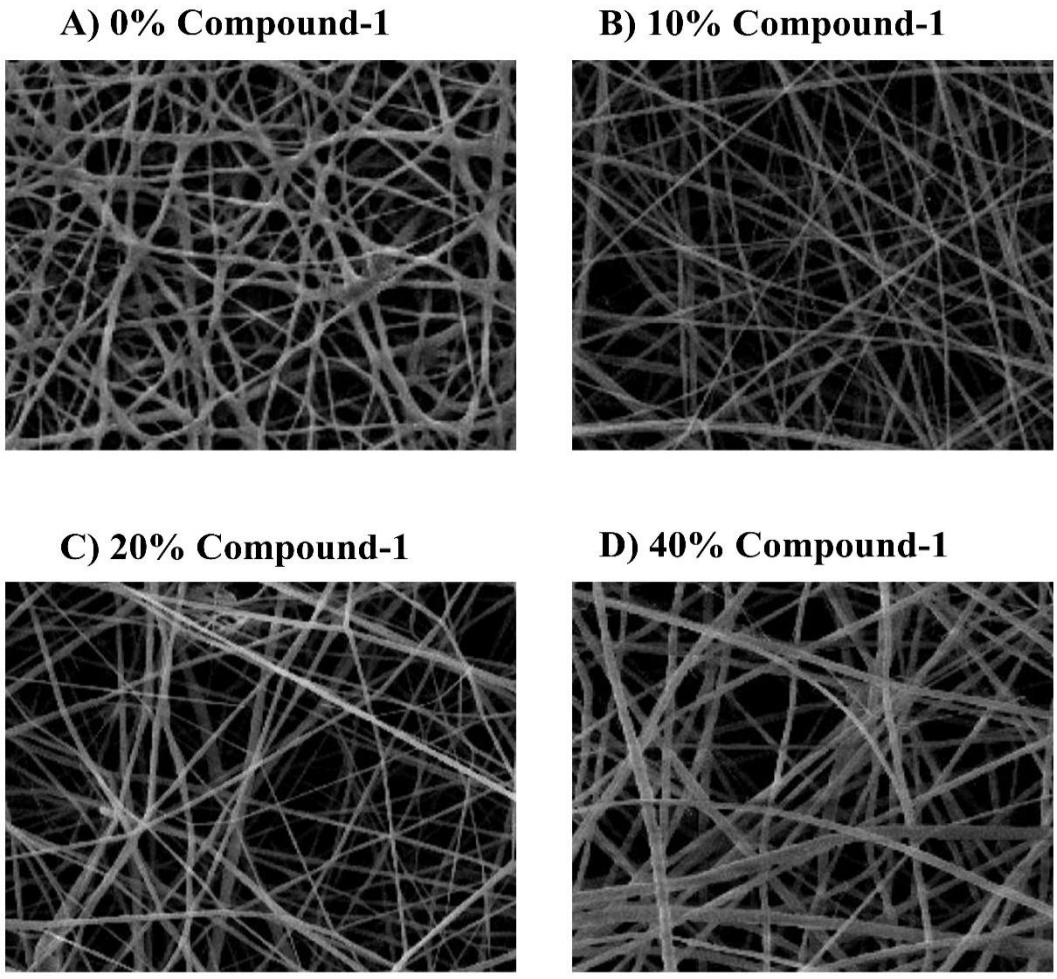

Figure 3: Morphology of fabricated starch nanofibers loaded with compound-1

3.2.2. Thermal stability of the nanofibers

The thermal stability analysis of the nanofibers represented a critical aspect of our investigation, providing valuable insights into the behavior of the composite materials. [13] This analysis was carried out using thermogravimetric analysis (TG), and the resulting weight loss thermogram and its corresponding first derivative thermogram are thoughtfully presented in Figure 4. Nanofibers devoid of compound-1 (0%) displayed a weight loss pattern closely resembling that of pure soluble potato starch. The initial phase involved the evaporation of moisture, an event typically occurring at around 100 °C. Subsequently, starch decomposition transpired in the temperature range of 260-330 °C, marking the second phase. In stark contrast, unencapsulated compound-1 exhibited a single-step weight loss phenomenon, manifesting at 310 °C, which is notably lower than its boiling point, estimated at approximately 374 °C. However, for nanofibers enriched with varying concentrations of compound-1 (10%, 20%, and 40%), a more intricate weight loss pattern emerged. The first phase mirrored the moisture evaporation seen in the previous case, transpiring around 100 °C. The second stage, observed within the temperature range of 250-340 °C, was likely attributed to the degradation of compound-1, showcasing a different behavior than its unbound form. The third phase involved starch decomposition, spanning the temperature range of 250-300 °C.

These findings affirm the effective encapsulation of compound-1 within the starch fibers, a process that subsequently contributes to the augmented thermal stability exhibited by the nanofibers loaded with compound-1. Such improved thermal stability is a promising attribute, particularly in scenarios where the engineered materials must withstand elevated temperatures while preserving their structural integrity, making them well-suited for applications in various biomedical and environmental contexts.

Journal of Chemical Health Risks

www.jchr.org

JCHR (2023) 13(4), 940-949 | ISSN:2251-6727

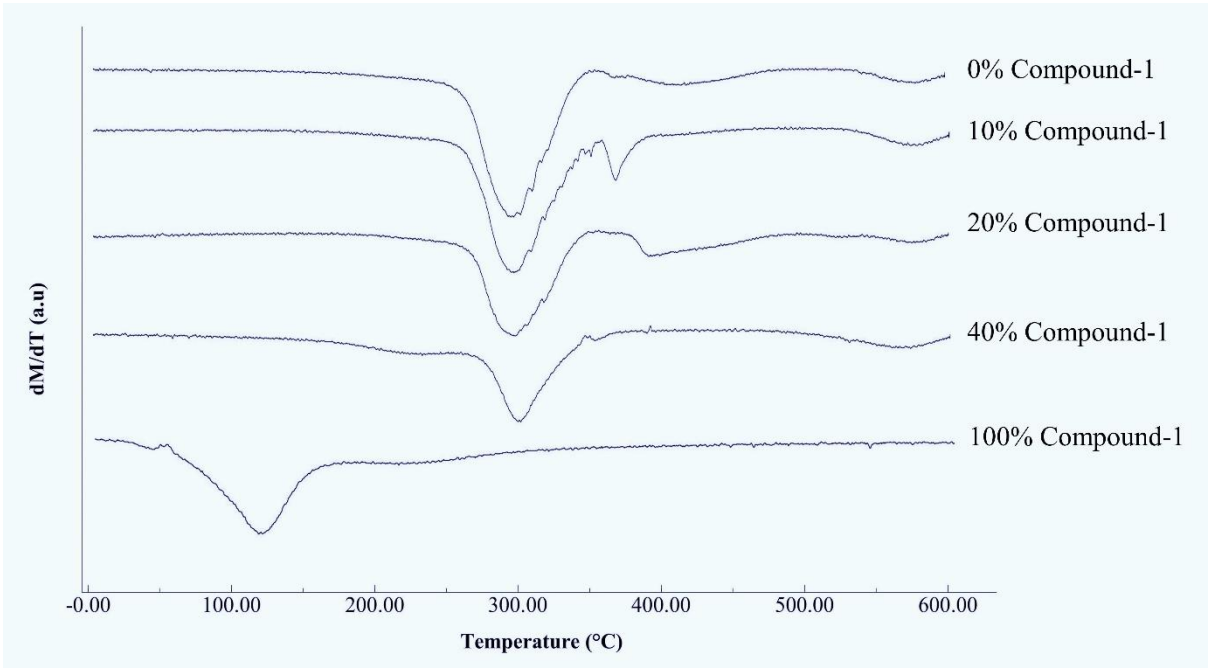

Figure 4: Thermogravimetric analysis of fabricated starch nanofibers loaded with compound-1

3.2.3. Fourier-transform infrared (FT-IR) spectroscopy analysis of the nanofibers

Figure 5 presents the fascinating FT-IR spectra of both the nanofibers and their individual constituents. These spectra offer a valuable window into the molecular interactions and characteristic vibrational patterns of the materials. In the FT-IR spectra, several distinctive bands were observed, primarily related to the chemical composition of soluble potato starch. Notably, the stretching vibrations of hydroxyl groups, both in intermolecular and intramolecular bonds, were evident in the spectra. The band at 2941 cm-1 can be attributed to the stretching of C-H bonds, underscoring the presence of carbon-hydrogen groups in the starch. Additionally, the band at 1641 cm-1 is characteristic of the presence of water molecules within the starch structure. The band at 1351 cm-1 represents the bending or deformation of C-O-H or CH2 groups, providing insights into the starch's molecular structure. Moreover, the bands at 1153 and 1020 cm-1 were associated with the stretching of single and double bonds, while the band around 920 cm-1 was likely indicative of glycosidic bonds present in glucose molecules, contributing to the overall starch structure.

In contrast, when it comes to the functional groups of compound-1, the FT-IR spectrum revealed distinct absorption bands characteristic of its molecular composition. The presence of the OH group was notably marked by a prominent absorption band at 3392 cm-1. Further inspection of the spectrum identified a C=C bond at 1612 cm-1, along with a C=O bond observed at 1714 cm-1, indicating the presence of double bonds and carbonyl groups in the compound. The C-H group was detected at multiple positions, specifically at 2929, 1462, and 1376 cm-1, further confirming the unique spectral signature of compound-1 within the nanofibers. These FT-IR findings provide robust evidence of the presence and interactions of compound-1 within the starch-based nanofibers. This knowledge is invaluable in elucidating the molecular dynamics of these materials and their potential contributions to various biomedical applications [14].

Journal of Chemical Health Risks

www.jchr.org

JCHR (2023) 13(4), 940-949 | ISSN:2251-6727

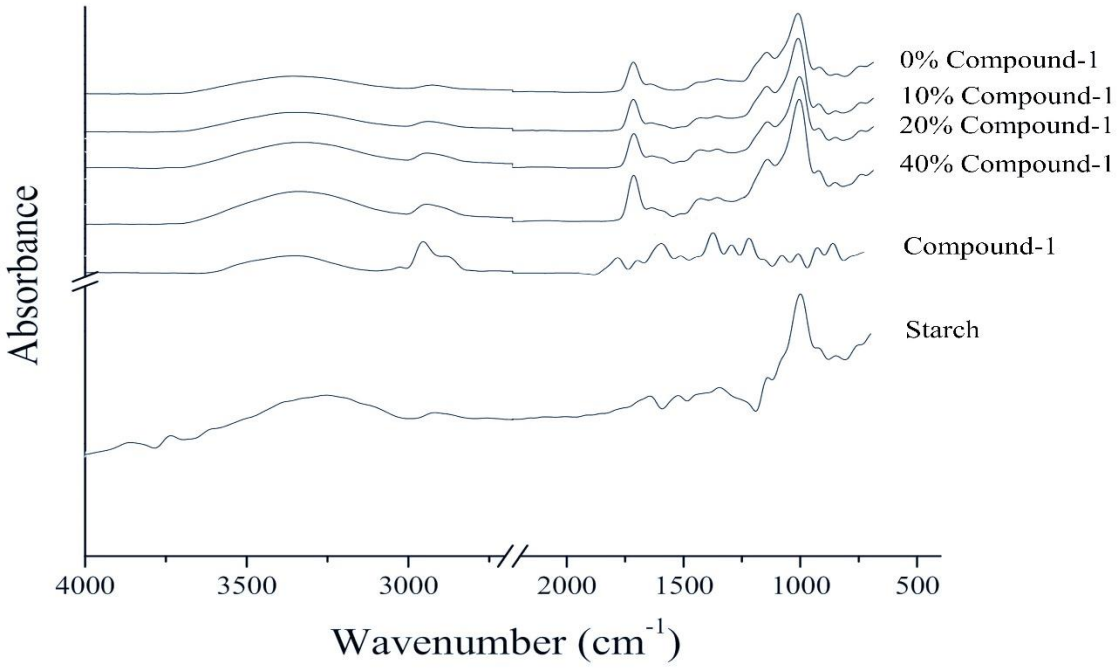

Figure 5: FT-IR analysis of fabricated starch nanofibers loaded with compound-1

3.3. Biological Characterization of fabricated nanofibers

3.3.1. Cell viability

The fundamental objective of an ideal wound dressing is to exhibit a high level of compatibility with the human body. This compatibility ensures that the wound dressing does not induce adverse reactions or harm to the surrounding tissue [15]. In our evaluation of the electrospun nanofibrous mats, we aimed to assess their biocompatibility, a critical factor in their suitability for various biomedical applications. To achieve this, we conducted an MTT (3-(4,5-dimethylthiazol-2-yl)-2,5-diphenyltetrazolium bromide) test using Human Keratinocytes, specifically HaCat Cells, as the model cell line. These cells were exposed to the electrospun nanofibrous mats for a duration of 24 hours, and the results are graphically represented in Figure 6. The outcomes of this biocompatibility test were notably encouraging. The electrospun nanofibrous mats demonstrated excellent cell viability and cytocompatibility, both of which are pivotal for their successful application in biomedical contexts. After the 24-hour exposure period, it was observed that the nanofibrous mats exhibited cell viability ranging from 100% to 140% when compared to the control sample, which was set at 100% as the baseline reference. This suggests that not only were the nanofibrous mats non-toxic to the cells, but they also promoted cell growth, resulting in viability exceeding the baseline.

An intriguing observation was that the nanofibrous mats containing starch, a significant component of the electrospun nanofibers, exhibited even higher cell viability when compared to those mats without starch [16]. This finding is particularly noteworthy, as it underscores the biocompatibility and potential benefits of the starch-based nanofibrous mats for tissue engineering and other biomedical applications. In summary, the results of the MTT test provide compelling evidence that the developed electrospun nanofibrous mats hold tremendous promise in the realm of biocompatibility, highlighting their potential to contribute positively to various biomedical applications, particularly in the field of tissue engineering [17].

Journal of Chemical Health Risks

www.jchr.org

JCHR (2023) 13(4), 940-949 | ISSN:2251-6727

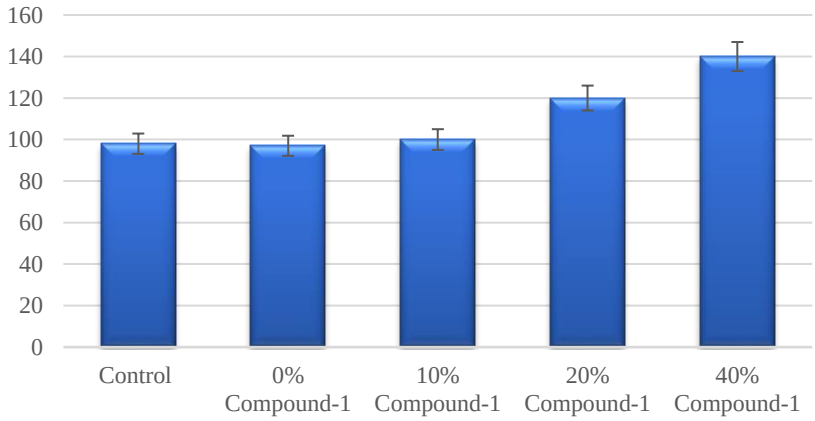

Figure 6: Cell viability of fabricated nanofibers on HaCat cells

4. CONCLUSION

In conclusion, this study has successfully demonstrated the fabrication and characterization of starch-based electrospun nanofibrous scaffolds incorporated with the bioactive compound, 12-(10-carboxydecanoyloxy)-12-oxododecanoic acid (Compound-1), sourced from *M. nudicaulis*. The comprehensive analysis of these nanofibers has provided valuable insights into their potential applications in the field of biomedical materials. The morphological analysis revealed that the incorporation of Compound-1 resulted in nanofibers with a consistent and uniform morphology, exhibiting average diameters within the range of 76 to 98 nm. Furthermore, the addition of Compound-1 enhanced the thermal stability of the nanofibers, as evidenced by thermogravimetric analysis (TGA). FT-IR spectroscopy confirmed the interactions between the starch matrix and Compound-1, indicating successful encapsulation. The cytotoxicity evaluation demonstrated that the developed nanofibrous scaffolds were highly biocompatible, with nanofibers containing starch exhibiting particularly high cell viability, emphasizing their potential for tissue engineering applications. These findings highlight the promise of the starch-based electrospun nanofibrous scaffolds enriched with Compound-1 as bioactive nanomaterials for various biomedical applications, particularly in the context of wound healing and tissue regeneration. However, further *in vitro* and *in vivo* studies are essential to validate and expand upon these initial observations and fully explore the potential of these innovative materials in clinical and therapeutic settings.

5. ACKNOWLEDGEMENT

We authors would like to express our sincere gratitude to the Department of Biotechnology, Annai College of Arts and Science, Kumbakonam, Tamil Nadu, India for completing this research work in such a fine manner.

7. CONFLICT OF INTEREST

Conflict of interest declared none

8. REFERENCES

1. Lavanya M, Krishnamoorthy R, Alshuniaber MA, Manoharadas S, Palanisamy CP, Veeraraghavan VP, Jayaraman S, Rajagopal P, Padmini R. Formulation, characterization and evaluation of gelatin-syringic acid/zinc oxide nanocomposite for its effective anticancer, antioxidant and anti-inflammatory activities. J King Saud Univ Sci. 2023; 35(8): 102909
2. Alugoju P, Palanisamy CP, Anthikapalli NVA, Jayaraman S, rasanskulab A, Chuchawankul S, Dyavaiah M, Tencomnao T. Exploring the anti-aging potential of natural products and plant extracts in budding yeast Saccharomyces cerevisiae: A review. F1000Research. 2023; 12: 1265.
3. Prasad M, Jayaraman S, Natarajan SR, Veeraraghavan VP, Krishnamoorthy R, Gatasheh MK, Palanisamy CP, Elrobh M. Piperine modulates IR/Akt/GLUT4 pathways to mitigate insulin resistance: Evidence from animal and computational studies. Int J Biol Macromol. 2023; 253: 127242.
4. Pei J, Palanisamy CP, Alugoju P, Anthikapalli NVA, Natarajan PM, Umapathy VR, Swamikannu B, Jayaraman S, Rajagopal P, Poompradub S. A comprehensive review on bio-based materials for

chronic diabetic wounds. Molecules. 2023; 28(2): 604.

5. Pei J, Umapathy VR, Vengadassalapathy S, Hussain SFJ, Rajagopal P, Jayaraman S, Veeraraghavan VP, Palanisamy CP, Gopinath K. A Review of the Potential Consequences of Pearl Millet (Pennisetum glaucum) for Diabetes Mellitus and Other Biomedical Applications. Nutrients. 2023; 14: 2932.
6. Palanisamy CP, Cui B, Zhang H, Gunasekaran VP, Ariyo AL, Jayaraman S, Rajagopal P, Long Q. A critical review on starch-based electrospun nanofibrous scaffolds for wound healing application. Int J Biol Macromol. 2022; 222: 1852-1860.
7. Raj SS, Palanisamy CP, Panagal M. (2021). Antioxidant, antimicrobial and cytotoxicity of nhexane extract from *Mollugo nudicaulis* Lam. *Bioinformation*. 17(5): 573-582.
8. Meganathan B, Palanisamy CP, Panagal M. (2021). Antioxidant, antimicrobial and cytotoxicity potential of n-hexane extract of *Cayratia trifolia* L. *Bioinformation*. 17(3): 452.
9. Palanisamy CP, Cui B, Zhang H, Jayaraman S, Muthukaliannan GK. (2020). A comprehensive review on corn starch-based nanomaterials: Properties, simulations, and applications. *Polymers.* 12(9): 2161.
10. Palanisamy CP, Fathima JHS, Sekar R, Rajagopal P, Jeyaraman S. (2021). MTT assay based inhibition analysis of A2780 cells proliferation using *Mollugo nudicaulis* Lam. extract with CXCR4 and HER2 expression. *Bioinformation*. 17(7): 705–709.
11. Palanisamy CP, Pethanan S, Vincent GG, Murugesan K, Ramachandran A, Sivanandam R, Panagal M. (2021). Chemotherapeutic potential of *Cayratia trifolia* L nhexane extract on A2780 cells. *Bioinformation.* 17(8): 710.
12. Perumal PC, Reddy CPK, Pratibha P, Sowmya S, Priyanga S, Devaki K, Ramkumar S, Gopalakrishnan VK. (2015). CXCR4 inhibitory activity analysis of linoleic acid isolated from ethanolic extract of *Cayratia trifolia* (L.): an molecular docking simulation. *Int J Pharmacog Phytochem Res*. 7(4): 781-784.
13. Perumal PC, Sowmya S, Velmurugan D, Sivaraman T, Gopalakrishnan VK. (2016). Assessment of dual inhibitory activity of epifriedelanol isolated from *Cayratia trifolia* against ovarian cancer. *Bangladesh J Pharmacol.* 11(2): 545-551
14. Sowmya S, Perumal PC, Anusooriya P, Vidya B, Pratibha P, Gopalakrishnan VK. (2015). *In vitro* antioxidant activity, in vivo skin irritation studies and HPTLC analysis of *Cayratia trifolia* (L.) Domin. *Int J Toxicol Pharmacol Res.* 7(1): 1-9.
15. Manimaran D, Elangovan N, Mani P, Subramanian K, Ali D, Alarifi S, Palanisamy CP, Zhang H, Rangasamy K, Palanisamy V, Mani R, Govarthanan K, Aruni W, Shanmugam R, Srinivasan GP, Kalirajan A. Isolongifolene-loaded chitosan nanoparticles synthesis and characterization for cancer treatment. Sci Rep. 2022; 12: 19250.
16. Palanisamy CP, Alugoju P, Jayaraman S, Poompradub S. Nigella sativa L. seed extracts promote wound healing progress by activating VEGF and PDGF signaling pathways: An in vitro and in silico study. F1000Research. 2023; 12: 436.
17. Palanisamy CP, Pei J, Alugoju P, Anthikapalli NVA, Jayaraman S, Veeraraghavan VP, Gopathy S, Roy JR, Janaki CS, Thalamati D, Mironescu M, Luo Q, Miao Y, Chai Y,Long Q. New strategies of neurodegenerative disease treatment with extracellular vesicles (EVs) derived from mesenchymal stem cells (MSCs). Theranostics. 2023; 13(12): 4138–4165.